Portland State University
PDXScholar

11-2012

Differential Effects of the Hydrophobic Surfactant Proteins on the Formation of Inverse Bicontinuous Cubic Phases

Mariya Chavarha
Oregon Health & Science University

Ryan W. Loney
Oregon Health & Science University

Kamlesh Kumar
Oregon Health & Science University

Shankar B. Rananavare
Portland State University, ranavas@pdx.edu

Stephen B. Hall
Oregon Health & Science University

Let us know how access to this document benefits you.

Follow this and additional works at: http://pdxscholar.library.pdx.edu/chem_fac

🌀 Part of the Biochemistry Commons, Chemistry Commons, and the Molecular Biology Commons

Citation Details

DIFFERENTIAL EFFECTS

OF THE HYDROPHOBIC SURFACTANT PROTEINS ON THE

FORMATION OF INVERSE BICONTINUOUS CUBIC PHASES

Mariya Chavarha[*], Ryan W. Loney[*], Kamlesh Kumar[*], Shankar B. Rananavare[†] and
Stephen B. Hall[*,‡]

[*]Departments of Biochemistry & Molecular Biology, Medicine, and Physiology &
Pharmacology, Oregon Health & Science University, Portland, OR 97239-3098
[†]Department of Chemistry, Portland State University, Portland, OR 97207

Running Title: Differential Effects of the Surfactant Proteins

[‡]To whom correspondence should be addressed:

1

Stephen B. Hall
Pulmonary & Critical Care Medicine
Mail Code UHN-67
Oregon Health & Science University
Portland, Oregon 97239-3098
email: sbh@ohsu.edu
Telephone: (503) 494-6667

ABSTRACT

Prior studies have shown that the biological mixture of the two hydrophobic surfactant proteins, SP-B and SP-C, produces faster adsorption of the surfactant lipids to an air/water interface, and that they induce 1-palmitoyl-2-oleoyl phosphatidylethanolamine (POPE) to form inverse bicontinuous cubic phases. SP-B has a much greater effect than SP-C on adsorption. If the two proteins induce formation of the bicontinuous structures and faster adsorption by similar mechanisms, then they should also have differential ability to form the cubic phases. To test this hypothesis, we measured small angle X-ray scattering on the individual proteins combined with POPE. SP-B replicated the dose-related ability of the combined proteins to induce the cubic phases at temperatures more than 25°C below the point at which POPE alone forms the curved inverse-hexagonal phase. With SP-C, diffraction from cubic structures was either absent or present only with larger amounts of protein at low intensities. The correlation between the structural effects of inducing curved structures and the functional effects on the rate of adsorption fits with the model in which SP-B promotes adsorption by facilitating formation of a negatively curved, rate-limiting intermediate structure.

INTRODUCTION

The hydrophobic surfactant proteins (SPs), SP-B and SP-C, accelerate the adsorption of vesicles containing the surfactant lipids to the alveolar air/water interface. With a clean interface, devoid of a film, the high surface tension can drive adsorption of vesicles containing only lipids (1). When surface tension subsequently approaches the equilibrium spreading value, adsorption requires the proteins (1). Any model of how the proteins achieve this function must explain two observations. First, the proteins promote adsorption whether restricted to the vesicles or to preexisting films at the interface (2,3). These results suggest that the proteins affect a rate-limiting structure that is equally accessible from both locations. Second, a variety of factors affect the kinetics of adsorption according to how they alter the curvature of phospholipid leaflets. The phosphatidylethanolamines (PEs) form the inverse hexagonal (H_{II}) phase, in which cylindrical monolayers have negative net curvature, with a concave hydrophilic surface. Gramicidin A enhances the negative net curvature of lipids in the H_{II} phase (4). Both PE and gramicidin A increase rates of adsorption (3,5-7). Lysophosphatidylcholine, which forms positively curved micelles, instead inhibits adsorption (7). These results collectively suggest a model of adsorption that is limited by formation of an hour-glass structure in which the outer leaflet of the vesicles forms two segments that bend back upon themselves to insert with the correct orientation into the air/water interface (8,9) (Fig. 1). Both the net (c_1+c_2) and Gaussian ($c_1 \cdot c_2$) curvatures of the monolayers in this kinetic intermediate would be negative. The proteins would accelerate adsorption by facilitating the formation of these rate-limiting structures.

Until recently, direct evidence that the proteins can affect curvature has been lacking. The surfactant lipids, with or without the proteins, form lamellar bilayers, which conceal any tendency of the lipids to curve. A change in the spontaneous curvature of the leaflets

induced by the proteins would be cancelled by the oppositely oriented, paired leaflet. Any change in the flexibility that would facilitate curvature in a transient intermediate during adsorption would remain unexpressed in the stable bilayer. The proposed effects of the surfactant proteins could be present in lamellar structures, but they would remain undetectable.

Lipids can form lamellar bilayers despite a tendency of their leaflets to curve because of a balance of energies. Curvature of a leaflet requires imperfect packing of acyl chains (10,11), which would be optimized in planar bilayers. If the energy of disrupted packing dominates the energy of bending away from the spontaneous curvature, then the leaflets remain lamellar. Introducing a more negative spontaneous curvature may shift the balance of energies, allowing the lipids to express effects on the tendency to curve that would otherwise be hidden. 1-palmitoyl-2-oleoyl phosphatidylethanolamine (POPE) forms the inverse hexagonal (H_{II}) phase above 71°C. At lower temperatures where POPE by itself exists as lamellar bilayers, the SPs induce formation of inverse bicontinuous cubic (Q_{II}) phases. In these continuously saddle-shaped bilayers, each monolayer has the negative net and Gaussian curvatures that characterize the hypothetical rate-limiting intermediate of adsorption (Fig. 1). These results show directly that the SPs can alter the curvature of lipid structures.

The advantages of substituting POPE for the surfactant lipids are mixed. The thermodynamically stable structures allow tests for effects on curvature that would be functionally important but elusive in transient intermediates, and inapparent in lamellar bilayers. The motivation, however, for forming the curved structures during adsorption of the surfactant lipids and with a PE would differ. The reduction in interfacial energy caused by the nascent film would drive formation of the hypothetical, curved, transient intermediate during adsorption of the surfactant lipids. The PEs instead form curved structures because of their effective molecular shape (12-14). Without an understanding

5

of how the proteins induce POPE to form the Q_{II} phases, the relevance of that structural effect to the adsorption of the surfactant lipids is uncertain.

The different abilities of the individual surfactant proteins to promote adsorption provide a simple test of the predicted relationship between structure and function. SP-B and SP-C both promote adsorption, but SP-B achieves its effect in much lower amounts (15). If induction of the Q_{II} phases by the combined proteins reflects effects that contribute to the acceleration of adsorption, then SP-B should promote the Q_{II} phases at much lower levels than SP-C. The studies reported here tested that hypothesis by using small angle X-ray scattering (SAXS) to determine how the individual proteins purified from calf surfactant affect the phase behavior of POPE.

MATERIALS AND METHODS

Materials:

1-palmitoyl-2-oleoyl phosphatidylethanolamine (POPE) and dioleoyl phosphatidylcholine (DOPC) were purchased from Avanti Polar Lipids (Alabaster, AL) and used without further characterization or purification. All reagents and solvents were ACS grade and obtained commercially from the following sources: NaCl, $CaCl_2$, chloroform and methanol (Mallinckrodt, Hazelwood, MO); UltraPure™ $Na_2EDTA-2H_2O$ (Invitrogen, Grand Island, NY); NaN_3 (Fluka Biochemika, Buchs, Switzerland); 4-(2-hydroxyethyl)-1-piperazineethanesulfonic acid (HEPES) (Sigma, St. Louis, MO). Water was processed and photo-oxidized with ultraviolet light using a NANOpure Diamond TOC-UV water-purification system (Barnstead/Thermolyne, Dubuque, IA). Extracted calf surfactant (calf lung surfactant extract, CLSE), provided by Dr. Edmund Egan (ONY, Inc., Amherst, NY), was obtained by lavaging calf lungs, recovering the surfactant aggregates by centrifugation, and extracting the hydrophobic constituents from the pelleted material (16).

Methods:

Separation of the surfactant proteins: The combined hydrophobic proteins were obtained from CLSE by gel permeation chromatography with a matrix of LH-20 (17,18). SP-B was separated from the combined proteins by licensed use of a patented procedure (19,20) based on the preferential partitioning of SP-B and SP-C into different phases formed by chloroform-methanol-water (21). The upper methanol-rich layer contained pure SP-B, which was dried by rotary evaporation and resuspended in chloroform-methanol (1:1, v:v). The lower chloroform-rich layer contained both proteins, which

7

were separated by gel permeation chromatography on a matrix of LH-60 (22,23) to yield the purified SP-C. Samples were eluted with a mobile phase of chloroform:methanol (1:1, v:v) driven by gravity and monitored by optical density at 240 and 280 nm (24). The extent of the different proteins in different fractions was determined by staining of proteins separated electrophoretically on polyacrylamide gels.

Biochemical characterization: The content of phospholipid was determined by measuring the amount of phosphate present (25). Total protein was determined with amido black on material precipitated by trichloroacetic acid (26). The molecular weights of separated proteins were established by electrophoresis on polyacrylamide gels containing sodium dodecyl sulphate (NuPAGE®, Invitrogen, Carlsbad, CA). Reduced samples used dithiothreitol at a final concentration of 50 mM. Proteins suspended in buffered lithium dodecyl sulfate were incubated at 70 ºC for 15 min, loaded on 4-12% gradient Bis/Tris gels, and run at a constant voltage of 200 V. The proteins were detected by incubation overnight with SYPRO® Ruby stain (Invitrogen, Carlsbad, CA).

Preparation of vesicles: The proteins were combined with the lipids in mixtures of chloroform and methanol, the ratio of which varied with the content of protein. Solvent was evaporated initially under a stream of nitrogen followed by incubation overnight at 2 mbar. For studies using small-angle x-ray scattering (SAXS), the lipid-protein mixtures were dispersed in 2 mM EDTA with 0.002% (w:w) NaN_3 to a final concentration of 50 mM phospholipid by hydrating overnight at 4 ºC followed by vigorous vortexing and cyclic freezing and thawing. The samples were transferred to capillaries (1.0 mm diameter, 0.01 mm wall thickness; "special glass"; Charles Supper, Natick, MA), centrifuged at 640 x g_{max} for 10 min, sealed with flame and epoxy, and stored at 4°C until use.

For studies of adsorption, vesicles were suspended in HS buffer (10 mM HEPES pH 7.0, 150 mM NaCl) to a final concentration of 16 mM phospholipid by vortexing, cyclic freeze-thawing, and extrusion 11 times at room temperature through a polycarbonate filter with pores of 100 nm (Whatman, Maidstone, U.K.). The average hydrodynamic radius, determined by dynamic light scattering (Protein Solutions Dynapro, Wyatt, Santa Barbara, CA), was 75 ± 25 nm for the vesicles containing the individual proteins, and 105 ± 32 nm with the combined proteins.

Adsorption: Kinetic measurements of adsorption monitored the fall in the surface tension of a captive bubble at ambient temperatures after injecting the samples containing the proteins combined with DOPC into a subphase of HSC (10 mM HEPES pH 7.0, 150 mM NaCl, 1.5 mM $CaCl_2$) to a final concentration of 0.5 mM phospholipid. The apparatus used to contain the captive bubble has been described previously (27). A computer analyzed the imaged profile of the bubble in real time to calculate surface tension and surface area, and used simple feedback to control infusion and withdrawal of buffer from the subphase by a syringe pump to hold area constant.

Small angle x-ray scattering: Diffraction was measured on beamline 1-4 at the Stanford Synchrotron Radiation Lightsource (SSRL). Up to 20 capillaries were mounted on an aluminum block, the temperature of which was controlled with water pumped from a circulating bath and monitored with an externally applied thermocouple. Block-temperatures were converted to sample-temperatures according to relationships established by melting a series of compounds with known melting points. Samples were equilibrated for at least 10 minutes at each temperature before exposure to radiation with a wavelength of 1.488 Å for 120 seconds. Angular dependence was calibrated using standard samples of silver behenate, cholesterol myristate, and lead stearate. The rings produced by powder diffraction were radially integrated using the program Fit2D (28) to obtain plots of intensity versus the scattering vector (q). Lamellar, hexagonal, and cubic

9

space groups were assigned according to the best fit of the measured values of q for the diffraction peaks to Miller indices allowed for the different structures (29,30). The slopes of the linear relationship between measured q and allowed values of $\sqrt{\ell^2+m^2+n^2}$ provided the lattice-constants (a_o) of the unit cells according to ($a_o = 2\pi/\text{slope}$) for the lamellar and cubic phases, and ($a_o = 4\pi / (\sqrt{3} \cdot \text{slope})$) for the hexagonal phase.

The results presented here were obtained using a single set of samples. Measurements with samples containing the same preparation of protein (SP-B; SP-C; or the combined proteins) were made at the same sequential temperatures. Three distinct sets of samples, with some measurements on beamline 4-2, produced comparable results, although in one case, samples with the larger amounts of SP-C did produce minor peaks with Q_{II} spacing. Intensities were well below the levels for samples with the combined proteins and with SP-B. Resuspension of the lipid-protein mixtures in HSC rather than EDTA produced no effect on the results.

RESULTS

Our samples used proteins that were separated from the surfactant lipids by established methods (17,18,23). The combined proteins provided by this procedure were then separated from each other using a licensed protocol based on the differential extraction of the individual proteins (19,20). Electrophoresis on gradient gels showed molecular weights of roughly 21 and 8 kDa for the unreduced and reduced samples of SP-B, respectively. These mobilities were consistent with results obtained previously for purified SP–B (24,31). Samples of SP-C produced a band at approximately 7 kDa that was unchanged by a reducing agent, consistent with the expected behavior of that monomeric peptide (32). The gels showed minimal cross-contamination of the purified samples by the other protein (Fig. 2).

Our studies used different lipids to demonstrate the effects of the proteins on adsorption and induction of the bicontinuous phases. The proteins induce phosphatidylethanolamines such as POPE to form Q_{II} phases (30). These phospholipids alone, however, adsorb rapidly without the proteins (3,5,6), presumably because of their tendency to form negatively curved structures. Therefore measurements of how the proteins affected adsorption used vesicles of DOPC, which by itself lowers surface tension slowly and incompletely, failing to reach the equilibrium surface tension of ~24 mN/m (1,3,7). When combined with equal amounts of protein (by weight), vesicles with SP-B reached equilibrium surface tension more rapidly than with SP-C (Fig. 3). The individual proteins produced an initial fall in surface tension that depended on concentration, with SP-C in some circumstances producing a greater effect. The final accelerated approach to the equilibrium surface tension, however, that is characteristic of adsorption by unilamellar vesicles of pulmonary surfactant (1) occurred earlier for SP-B.

11

These results agreed with the previously published finding (15) that SP-B is more effective in promoting adsorption than SP-C.

Measurements of SAXS for POPE alone and with the combined proteins produced expected results. POPE by itself converted from one lamellar spacing to another between 21 and 30°C, and to a hexagonal phase beginning at 70°C (Fig. 4,5). These results were consistent with the calorimetrically determined transitions from $L_{\beta'}$ to L_{α} phases at 26°C (33), and from L_{α} to H_{II} at 71°C (34). The combined proteins induced diffraction at intervals expected from cubic space groups (Fig. 4,5). In samples containing 0.01% SP, diffraction consistent with $Pn\overline{3}m$ structures began at 61°C; $Im\overline{3}m$ spacing emerged at 70°C (Fig. 4,5). Increasing amounts of protein lowered the temperature at which the cubic phases first appeared, reaching 30°C at 5% SP (Fig. 5). The hexagonal phase, which coexisted with the Q_{II} phases in samples containing small amounts of protein, was absent at > 0.03% SP (Fig. 5). Results with the combined proteins suggested a dose-dependent decrease in the lattice-constant of the Q_{II} structures that had not been apparent from our previous measurements (Fig. 6A,C). In other respects, our findings here confirmed the results reported previously for the combined proteins with POPE (30).

SP-B alone produced similar effects. Like the combined proteins, SP-B produced no change in either the transition-temperatures of the lamellar phases or their lattice-constants. Small amounts of SP-B, similar to the levels of the combined proteins that achieved the same effect, induced the Q_{II} phases (Fig. 4-6). Diffraction for both $Pn\overline{3}m$ and $Im\overline{3}m$ space groups appeared with as little as 0.03% SP-B (Figs. 4-6). Like the combined proteins, greater amounts of SP-B lowered the temperature at which the Q_{II} phases appeared, reaching 43°C for the $Im\overline{3}m$ space group at 5.0% SP-B. Results with SP-B also suggested the dose-dependent decrease in the lattice-constant of the Q_{II} structures, particularly at the lower temperatures (Fig. 6). In these several respects, SP-B replicated the effects of the combined proteins on the phase behavior of POPE.

In contrast, SP-C produced little change in the behavior of the lipids. The protein in concentrations from 0.01 - 1.0% had no effect on the transition-temperatures or the lattice-constant for the lamellar or the H_{II} phases. SP-C either failed to produce any evidence of the Q_{II} phases (Fig. 4,5), or, with other preparations not shown here, produced only traces of Q_{II} diffraction with samples containing the larger amounts of protein. For a single preparation, the hexagonal lattice-constant at 3% SP-C also decreased from the value with lower amounts of protein, but for the other samples, the value remained invariant. Any ability of SP-C to alter the structure of the lipids, if present, was greatly reduced relative to SP-B.

DISCUSSION

The studies reported here provide a simple test of a model for how the hydrophobic surfactant proteins promote adsorption. The model predicts that the proteins facilitate formation of an hourglass-shaped stalk that connects the adsorbing vesicle to the air/water interface (Fig. 1). Consistent with the model, low amounts of the combined proteins induce POPE to form Q_{II} phases, in which each leaflet has the negative net and Gaussian curvatures predicted for the rate-limiting kinetic intermediate. The efficiencies with which the individual proteins promote adsorption are different. If induction of the Q_{II} phases reflects the same mechanisms that lead to faster adsorption, then the two proteins should have different abilities to generate the Q_{II} structures.

Our results confirm that hypothesis. In the same low amounts as the combined proteins, SP-B induces formation of the Q_{II} phases. SP-C, which has much less effect on adsorption, either fails at all levels to generate cubic diffraction or induces only low intensity peaks with higher levels of the protein. Our results indicate that, like adsorption, the ability of the combined proteins to induce formation of the Q_{II} phases reflects primarily the effects of SP-B. These findings establish the correlation between the structural and functional effects of the two proteins predicted by the model.

These results fit with the available information on the structure of the two proteins and with the behavior of other lipid-protein mixtures. The primary structure of SP-C consists mostly of a hydrophobic sequence that would generate a transmembrane helix (32). The sequence of SP-B instead suggests a series of amphipathic helices that should insert into the face of a bilayer (35). Although proposals concerning how the two monomeric peptides in SP-B fit into the disulfide-linked dimer have been conspicuously absent (36), vibrational spectroscopy supports the extent of amphipathic helices suggested by the sequence (37). Although some peptides that induce inverse cubic phases (38) form

14

transmembrane helices, peptides with that activity generally form amphipathic helices (39-44).

The correlation between the structural and functional effects of the proteins supports the relevance of the Q_{II} phases to adsorption. That relationship still requires a common mechanism that could explain how SP-B can promote both the Q_{II} phases and the hypothetical curved intermediate. Important aspects of both the lipids and the structures are different. The magnitude of spontaneous curvature should be much less for the surfactant lipids, which are dominated by constituents (45) that by themselves form only lamellar phases, than for POPE, which forms the H_{II} phase above 71 °C (34). The individual lipid leaflets are unpaired in the hypothetical kinetic intermediate, in contrast to the bilayers of the Q_{II} phase. The motivation for forming the two curved structures would differ, and only the Q_{II} phase would represent an equilibrium configuration. Given these differences, the mechanism by which SP-B could induce the distinct lipids to form the two structures requires careful consideration.

SP-B may induce formation of the Q_{II} phases by effects that are thermodynamic or kinetic. For thermodynamic processes, the energy of the curved structure includes contributions from bending, the packing of acyl chains, and the interaction between adjacent bilayers (46,47). Two of these are probably unimportant. Prior calculations suggest that the difference between the energy per unit-area of chain-packing for lamellar and Q_{II} phases should be relatively similar (48-50). This limited difference provides little basis for SP-B to favor the curved structures by affecting chain-packing. Effects on the energy of interaction between adjacent bilayers also seem unlikely here. Although our studies included no attempts to measure that energy directly, the absence of any effect by SP-B on the spacing of the lamellar phases argues against a change in the interaction energy. The induction of the Q_{II} phases by SP-B should reflect effects on the energy of bending.

15

Expressions for the energy of bending indicate the conditions necessary to form the Q_{II} phases. For limited bending of a thin sheet, the energy per unit-area, g, or energy-density, includes independent terms from simple-splay and saddle-splay curvatures. In each case, the deviation from the spontaneous configuration determines the contribution, modified by an elastic modulus (51):

$$g = \tfrac{1}{2}\kappa(c_1 + c_2 - c_o)^2 + \overline{\kappa}c_1c_2 \qquad [1]$$

κ and $\overline{\kappa}$ are the moduli of simple-splay and Gaussian curvatures, respectively. c_o is the spontaneous curvature of simple-splay curvature adopted in the absence of an applied force; spontaneous Gaussian curvature is unknown. With symmetric bilayers that contain identical, oppositely oriented monolayers, $c_o^b = 0$. (The superscripts [b] and [m] indicate variables for the bilayer and monolayer, respectively). In the Q_{II} phases, the midpoint of the bilayer falls along a minimal surface, at which $c_1^b = -c_2^b$, eliminating any contribution from simple-splay curvature. Because $c_1^b \cdot c_2^b < 0$, the negative energy that would spontaneously produce the Q_{II} phases requires $\overline{\kappa}^b > 0$ (52-54). If SP-B induces POPE to form Q_{II} phases by a thermodynamic effect, then the protein acts by increasing $\overline{\kappa}^b$ to a positive value.

The changes that induce Q_{II} phases in bilayers should extend to the monolayers of the hypothetical intermediate. For monolayers in which a distance, δ, separates the neutral plane, at which the energies of stretching and curvature uncouple during bending, from the midpoint of the bilayer (47,54-56),

$$\overline{\kappa}^b = 2(\overline{\kappa}^m - 2\kappa^m\delta c_o^m) \qquad [2]$$

Formation of a Q_{II} phase therefore requires

$$\overline{\kappa}^m - 2\kappa^m\delta c_o^m > 0 \qquad [3]$$

Although we performed no direct measurements of c_o^m or δ, the invariance of the H_{II}-lattice at different levels of SP-B (Fig. 5) make changes in c_o^m or δ less likely, and suggests that SP-B achieves its effect by altering one or both moduli of curvature. The important point, however, is simply that the changes in bilayers reflect alterations in the characteristics of their monolayers. Whatever combination of changes in the parameters of the monolayers induce lamellar bilayers to form Q_{II} structures should facilitate bending of the individual leaflets in the hypothetical intermediate that would determine the rate of adsorption (Fig. 1).

The values of $\bar{\kappa}^m$, κ^m, and c_o^m originate in a common source. The lateral stress-profile of the monolayer determines each of these parameters (52,53,57-61). Without the proteins, the stress-profile for POPE and the surfactant lipids should differ. SP-B induces POPE to form the Q_{II} phase by shifting the profile. If SP-B generates analogous shifts in the profile for the surfactant lipids, the protein would produce comparable changes in the tendency of those lipids to curve. This common mechanism reasonably explains how SP-B could facilitate formation of the distinct curved structures by the different lipids.

In addition to these thermodynamic mechanisms, SP-B could also induce Q_{II} phases by kinetic effects. This possibility is supported by the behavior of pure lipids that form curved structures. Generally these lipids convert during heating directly from L_α to the H_{II} phase. During repeated cycling through the L_α-H_{II} transition, however, the Q_{II} phases can emerge below the temperature of the H_{II} phase (62). This observation suggests that the bicontinuous phases may represent the most stable forms at intermediate temperatures, above the range of the L_α phase and below H_{II}, but that these structures are kinetically inaccessible. The ability of SP-B to induce the Q_{II} phases and promote faster adsorption could reflect its ability to provide a lower-energy pathway to the curved structures rather than an effect on their stability.

17

In summary, SP-B, but not SP-C, replicates the ability of the combined proteins to induce POPE to form Q_{II} phases more than 25°C below the L_{α}-H_{II} transition for the lipid alone. These results fit with a model that explains the much greater ability of SP-B than SP-C to promote faster adsorption in terms of effects on a rate-limiting structure in which lipid leaflets have negative net and Gaussian curvatures.

ACKNOWLEDGMENTS

REFERENCES

1.   Loney, R.W., W.R. Anyan, S.C. Biswas, S.B. Rananavare, and S.B. Hall. 2011. The accelerated late adsorption of pulmonary surfactant. Langmuir 27:4857-4866.

2.   Oosterlaken-Dijksterhuis, M.A., H.P. Haagsman, L.M.G. van Golde, and R.A. Demel. 1991. Interaction of lipid vesicles with monomolecular layers containing lung surfactant proteins SP-B or SP-C. Biochemistry 30:8276-8281.

3.   Biswas, S.C., S.B. Rananavare, and S.B. Hall. 2005. Effects of gramicidin-A on the adsorption of phospholipids to the air-water interface. Biochim. Biophys. Acta 1717:41-49.

4.   Szule, J.A. and R.P. Rand. 2003. The effects of gramicidin on the structure of phospholipid assemblies. Biophys. J. 85:1702-1712.

5.   Yu, S.-H., P.G.R. Harding, and F. Possmayer. 1984. Artificial pulmonary surfactant. Potential role for hexagonal H_{II} phase in the formation of a surface-active monolayer. Biochim. Biophys. Acta 776:37-47.

6.   Perkins, W.R., R.B. Dause, R.A. Parente, S.R. Minchey, K.C. Neuman, S.M. Gruner, T.F. Taraschi, and A.S. Janoff. 1996. Role of lipid polymorphism in pulmonary surfactant. Science 273:330-332.

7.   Biswas, S.C., S.B. Rananavare, and S.B. Hall. 2007. Differential effects of lysophosphatidylcholine on the adsorption of phospholipids to an air/water interface. Biophys. J. 92:493-501.

8.   Walters, R.W., R.R. Jenq, and S.B. Hall. 2000. Distinct steps in the adsorption of pulmonary surfactant to an air-liquid interface. Biophys. J. 78:257-266.

9.   Klenz, U., M. Saleem, M.C. Meyer, and H.J. Galla. 2008. Influence of lipid saturation grade and headgroup charge: a refined lung surfactant adsorption model. Biophys. J. 95:699-709.

10.   Charvolin, J. and J.F. Sadoc. 1987. Periodic systems of frustrated fluid films and <<bicontinuous>> cubic structures in liquid crystals. J. Phys. (Paris) 48:1559-1569.

11.   Gruner, S.M. 1989. Stability of lyotropic phases with curved interfaces. J. Phys. Chem. 93:7562-7570.

12.   Tanford, C. 1973. The Hydrophobic Effect: Formation of Micelles and Biological Membranes. New York: Wiley.

13.   Israelachvili, J.N., S. Marcelja, and R.G. Horn. 1980. Physical principles of membrane organization. Q. Rev. Biophys. 13:121-200.

14.   Israelachvili, J.N., D.J. Mitchell, and B.W. Ninham. 1976. Theory of self-assembly of hydrocarbon amphiphiles into micelles and bilayers. J. Chem. Soc., Faraday Trans. 2 72:1525-1568.

15.   Wang, Z., O. Gurel, J.E. Baatz, and R.H. Notter. 1996. Differential activity and lack of synergy of lung surfactant proteins SP-B and SP-C in interactions with phospholipids. J. Lipid Res. 37:1749-1760.

16.   Notter, R.H., J.N. Finkelstein, and R.D. Taubold. 1983. Comparative adsorption of natural lung surfactant, extracted phospholipids, and artificial phospholipid mixtures to the air-water interface. Chem. Phys. Lipids 33:67-80.

17.   Takahashi, A. and T. Fujiwara. 1986. Proteolipid in bovine lung surfactant: its role in surfactant function. Biochem. Biophys. Res. Comm. 135:527-532.

18.   Hall, S.B., Z. Wang, and R.H. Notter. 1994. Separation of subfractions of the hydrophobic components of calf lung surfactant. J. Lipid Res. 35:1386-1394.

19.   Egan, E.A., L.M. Hlavaty, and B.A. Holm; ONY, Inc., assignee. 2000. Compositions and methods for isolating lung surfactant hydrophobic proteins SP-B and SP-C. U.S. patent 6,020,307.

20.   Egan, E.A., L.M. Hlavaty, and B.A. Holm; Ony, Inc., assignee. 2002. Compositions and methods for isolating lung surfactant hydrophobic proteins SP-B and SP-C. U.S. patent 6,458,759.

21.   Bligh, E. and W. Dyer. 1959. A rapid method of total lipid extraction and purification. Can. J. Biochem. 37:911-917.

22.   Warr, R.G., S. Hawgood, D.I. Buckley, T.M. Crisp, J. Schilling, B.J. Benson, P.L. Ballard, J.A. Clements, and R.T. White. 1987. Low molecular weight human pulmonary surfactant protein (SP5): isolation, characterization, and cDNA and amino acid sequences. Proc. Natl. Acad. Sci. U.S.A. 84:7915-7919.

23.   Curstedt, T., H. Jornvall, B. Robertson, T. Bergman, and P. Berggren. 1987. Two hydrophobic low-molecular-mass protein fractions of pulmonary surfactant. Characterization and biophysical activity. Eur. J. Biochem. 168:255-262.

24.   Pérez-Gil, J., A. Cruz, and C. Casals. 1993. Solubility of hydrophobic surfactant proteins in organic solvent/water mixtures. Structural studies on SP-B and SP-C in aqueous organic solvents and lipids. Biochim. Biophys. Acta 1168:261-270.

25.   Ames, B.N. 1966. Assay of inorganic phosphate, total phosphate and phosphatases. Meth. Enzymol. VIII:115-118.

26.   Kaplan, R.S. and P.L. Pedersen. 1985. Determination of microgram quantities of protein in the presence of milligram levels of lipid with amido black 10B. Anal. Biochem. 150:97-104.

27.   Smith, E.C., T.G. Laderas, J.M. Crane, and S.B. Hall. 2004. Persistence of metastability after expansion of a supercompressed fluid monolayer. Langmuir 20:4945-4953.

28.   Hammersley, A.P., S.O. Svensson, M. Hanfland, A.N. Fitch, and D. Hausermann. 1996. Two-dimensional detector software: From real detector to idealised image or two-theta scan. High Pressure Res. 14:235 - 248.

29.   Sun, R.G. and J. Zhang. 2004. The cubic phase of phosphatidylethanolamine film by small angle x-ray scattering. J. Phys. D: Appl. Phys. 37:463-467.

30.   Chavarha, M., H. Khoojinian, L.E. Schulwitz, Jr., S.C. Biswas, S.B. Rananavare, and S.B. Hall. 2010. Hydrophobic surfactant proteins induce a phosphatidylethanolamine to form cubic phases. Biophys. J. 98:1549-1557.

31.   Baatz, J.E., Y. Zou, J.T. Cox, Z.D. Wang, and R.H. Notter. 2001. High-yield purification of lung surfactant proteins SP-B and SP-C and the effects on surface activity. Protein Expr. Purif. 23:180-190.

32.   Johansson, J., T. Curstedt, B. Robertson, and H. Jörnvall. 1988. Size and structure of the hydrophobic low molecular weight surfactant-associated polypeptide. Biochemistry 27:3544-3547.

33.   Brown, P.M., J. Steers, S.W. Hui, P.L. Yeagle, and J.R. Silvius. 1986. Role of head group structure in the phase behavior of amino phospholipids. 2. Lamellar and nonlamellar phases of unsaturated phosphatidylethanolamine analogues. Biochemistry 25:4259-4267.

34.   Epand, R.M. and R. Bottega. 1987. Modulation of the phase transition behavior of phosphatidylethanolamine by cholesterol and oxysterols. Biochemistry 26:1820-1825.

35.   Curstedt, T., J. Johansson, J. Barros-Soderling, B. Robertson, G. Nilsson, M. Westberg, and H. Jornvall. 1988. Low-molecular-mass surfactant protein type 1. The primary structure of a hydrophobic 8-kDa polypeptide with eight half-cystine residues. Eur. J. Biochem. 172:521-525.

36.   Whitsett, J.A. and T.E. Weaver. 2002. Hydrophobic surfactant proteins in lung function and disease. New Engl. J. Med. 347:2141-2148.

37.   Vandenbussche, G., A. Clercx, M. Clercx, T. Curstedt, J. Johansson, H. Jornvall, and J.M. Ruysschaert. 1992. Secondary structure and orientation of the surfactant protein SP-B in a lipid environment. Biochemistry 31:9169-9176.

38.   Siegel, D.P., V. Cherezov, D.V. Greathouse, R.E. Koeppe, 2nd, J.A. Killian, and M. Caffrey. 2006. Transmembrane peptides stabilize inverted cubic phases in a biphasic length-dependent manner: implications for protein-induced membrane fusion. Biophys. J. 90:200-211.

39.   Angelova, A., R. Ionov, M.H. Koch, and G. Rapp. 2000. Interaction of the peptide antibiotic alamethicin with bilayer- and non-bilayer-forming lipids: influence of increasing alamethicin concentration on the lipids supramolecular structures. Arch. Biochem. Biophys. 378:93-106.

40.   Kamo, T., M. Nakano, Y. Kuroda, and T. Handa. 2006. Effects of an amphipathic α-helical peptide on lateral pressure and water penetration in phosphatidylcholine and monoolein mixed membranes. J. Phys. Chem. B 110:24987-24992.

41.   Hickel, A., S. Danner-Pongratz, H. Amenitsch, G. Degovics, M. Rappolt, K. Lohner, and G. Pabst. 2008. Influence of antimicrobial peptides on the formation of nonlamellar lipid mesophases. Biochim. Biophys. Acta 1778:2325-2333.

42. Zweytick, D., S. Tumer, S.E. Blondelle, and K. Lohner. 2008. Membrane curvature stress and antibacterial activity of lactoferricin derivatives. Biochem. Biophys. Res. Comm. 369:395-400.

43. Fuhrmans, M., V. Knecht, and S.J. Marrink. 2009. A single bicontinuous cubic phase induced by fusion peptides. J. Am. Chem. Soc. 131:9166-9167.

44. Keller, S.L., S.M. Gruner, and K. Gawrisch. 1996. Small concentrations of alamethicin induce a cubic phase in bulk phosphatidylethanolamine mixtures. Biochim. Biophys. Acta 1278:241-246.

45. Kahn, M.C., G.J. Anderson, W.R. Anyan, and S.B. Hall. 1995. Phosphatidylcholine molecular-species of calf lung surfactant. Am. J. Physiol. 13:L567-L573.

46. Kirk, G.L., S.M. Gruner, and D.L. Stein. 1984. A thermodynamic model of the lamellar to inverse hexagonal phase transition of lipid membrane-water systems. Biochemistry 23:1093-1102.

47. Shearman, G.C., O. Ces, R.H. Templer, and J.M. Seddon. 2006. Inverse lyotropic phases of lipids and membrane curvature. J. Phys.-Condens. Mat. 18:S1105-S1124.

48. Anderson, D.M., S.M. Gruner, and S. Leibler. 1988. Geometrical aspects of the frustration in the cubic phases of lyotropic liquid crystals. Proc. Natl. Acad. Sci. U.S.A. 85:5364-5368.

49. Templer, R.H., J.M. Seddon, P.M. Duesing, R. Winter, and J. Erbes. 1998. Modeling the phase behavior of the inverse hexagonal and inverse bicontinuous cubic phases in 2:1 fatty acid/phosphatidylcholine mixtures. J. Phys. Chem. B 102:7262-7271.

50. Shearman, G.C., B.J. Khoo, M.L. Motherwell, K.A. Brakke, O. Ces, C.E. Conn, J.M. Seddon, and R.H. Templer. 2007. Calculations of and evidence for chain packing stress in inverse lyotropic bicontinuous cubic phases. Langmuir 23:7276-7285.

51. Helfrich, W. 1973. Elastic properties of lipid bilayers: theory and possible experiments. Z. Naturforsch. 28:693-703.

52. Helfrich, W. and W. Harbich. 1987. Equilibrium configurations of fluid membranes. In Physics of Amphiphilic Layers : proceedings of the workshop, Les Houches, France, February 10-19, 1987. J. Meunier, D. Langevin, and N. Boccara, editors. Springer-Verlag. Berlin. 58-63.

53. Helfrich, W. 1994. Lyotropic lamellar phases. J. Phys.-Condens. Mat. 6:A79-A92.

54. Siegel, D.P. and M.M. Kozlov. 2004. The gaussian curvature elastic modulus of N-monomethylated dioleoylphosphatidylethanolamine: relevance to membrane fusion and lipid phase behavior. Biophys. J. 87:366-374.

55. Lorenzen, S., R.M. Servuss, and W. Helfrich. 1986. Elastic torques about membrane edges: a study of pierced egg lecithin vesicles. Biophys. J. 50:565-572.

56.   Helfrich, W. and H. Rennscuh. 1990. Landau theory of the lamellar-to-cubic phase transition. J. Phys. Colloques 51:C7,189-195.

57.   Harbich, W., R.M. Servuss, and W. Helfrich. 1978. Passages in lecithin-water systems. Z. Naturforsch. 33a:1013-1017.

58.   Petrov, A.G., M.D. Mitov, and A. Derzhanski. 1978. Saddle splay instability in lipid bilayers. Phys. Lett. A 65:374-376.

59.   Helfrich, W. 1981. Amphiphilic mesophases made of defects. In Physique des dÈfauts : les Houches, session XXXV, 28 Juillet-29 Ao°t 1980. R. Balian, M. Kléman, and J.-P. Poirier, editors. North-Holland. Amsterdam; New York; Oxford. 716-755.

60.   Helfrich, W. 1990. Elasticity and thermal undulations of fluid films of amphiphiles. In Liquides aux Interfaces = Liquids at Interfaces. J. Charvolin, J.F. Joanny, and J. Zinn-Justin, editors. North-Holland. Amsterdam. 209-237.

61.   Seddon, J.M. 1990. Structure of the inverted hexagonal (H_{II}) phase, and non-lamellar phase transitions of lipids. Biochim. Biophys. Acta 1031:1-69.

62.   Shyamsunder, E., S.M. Gruner, M.W. Tate, D.C. Turner, P.T. So, and C.P. Tilcock. 1988. Observation of inverted cubic phase in hydrated dioleoylphosphatidylethanolamine membranes. Biochemistry 27:2332-2336.

FIGURE LEGENDS

1. Hypothetical structure of the kinetic intermediate that limits the rate of adsorption. The outer leaflet of the vesicle must invert to insert into the air/water interface with the correct orientation. The two principal curvatures of the intermediate structure would have opposite signs. In the plane perpendicular to the interface, the curvature of the leaflet ($c_1 \equiv 1/R_1$), with its concave hydrophilic face, would by convention be negative. In the plane parallel to the interface, the curvature ($c_2 \equiv 1/R_2$) of the convex hydrophilic face would be positive.

2. Electrophoretic separation of the hydrophobic surfactant proteins. Labels indicate lanes containing the following samples: the combined proteins collected together from CLSE by gel permeation chromatography on a matrix of LH-20 (SP); SP-B separated from the SP by licensed use of a patented extraction procedure (SP-B); SP-C purified by extraction of the combined proteins followed by gel permeation chromatography on LH-60 (SP-C); molecular-weight markers (MWM) with the indicated molecular weights (Mol. Wt.). A. Non-reducing lanes: samples without dithiothreitol. B. Reducing lanes: samples containing 50 mM dithiothreitol.

3. Adsorption of DOPC combined with the different surfactant proteins. Concentrated aliquots of protein-DOPC mixtures in HS were injected into a subphase of HSC at ambient temperatures below a captive bubble. The shape of the bubble provided the basis for calculating surface tension and surface area. Surface area was held constant using a computer-controlled syringe pump to infuse and withdraw buffer from the subphase. The time-axis is split to illustrate the different kinetics for adsorption of samples with SP-B and SP-C.

4. Diffraction from POPE with the different surfactant proteins at different temperatures. Samples, dispersed in 2 mM EDTA, contained POPE with: A. the copurified hydrophobic proteins; B. SP-B; C. SP-C. Labels in each panel indicate the amount of protein (%, w:w) per phospholipid. The graph omits data at additional temperatures and amounts of protein for clarity of presentation.

5. Lattice-constant (a_o) of structures with the different space groups at different temperatures. Q_{II}^P and Q_{II}^D indicate bicontinuous cubic phases corresponding to the primitive (space group $Im\overline{3}m$) and diamond ($Pn\overline{3}m$) infinitely periodic minimal surfaces, respectively. POPE with: A. the copurified SP-B/C; B. SP-B; C. SP-C.

6. Dose-response of the lattice-constants for the Q_{II} phases to variable amounts of the combined proteins and SP-B. Panels indicate the lattice-constant of structures with $Pn\overline{3}m$ or $Im\overline{3}m$ space groups for POPE mixed with either the combined proteins or SP-B. The graphs omit results at 30-43°C because the range of protein concentrations that produced the Q_{II} phases at those temperatures was limited.
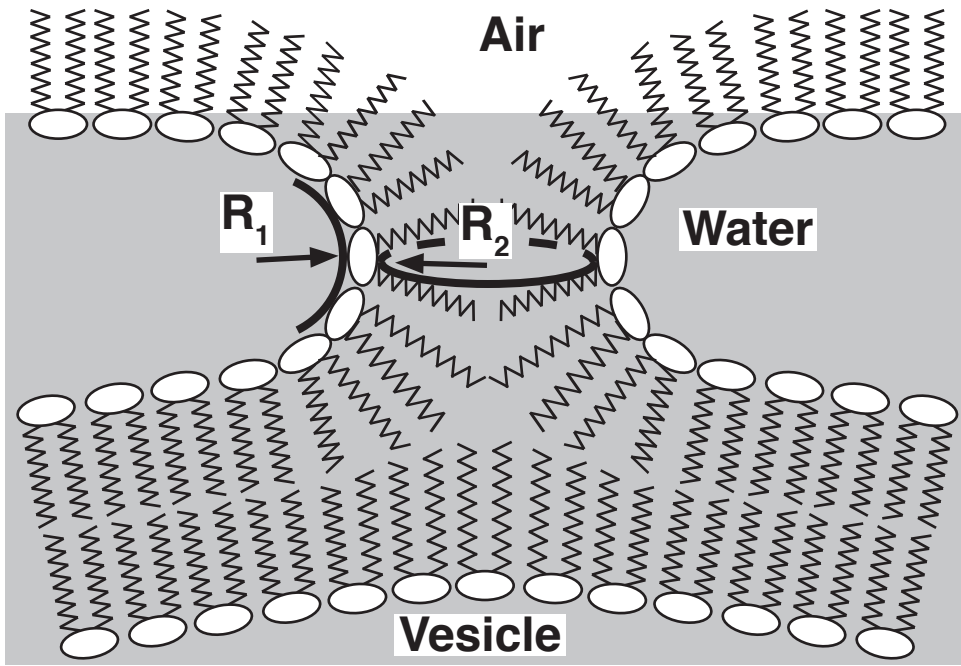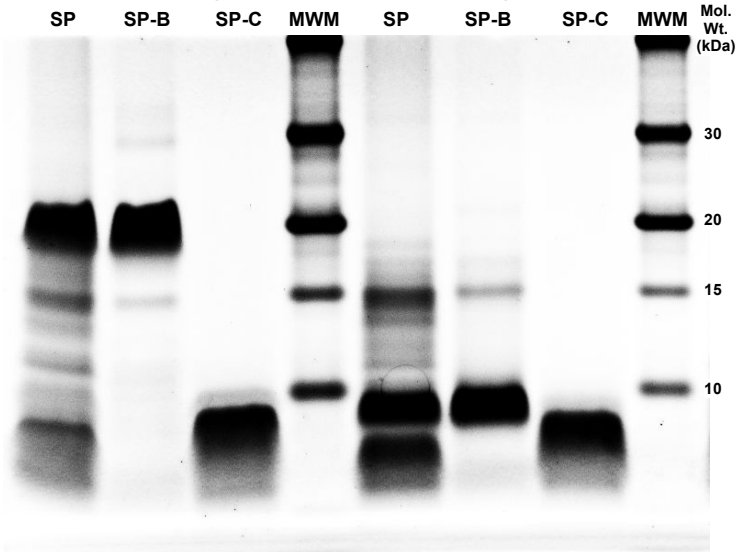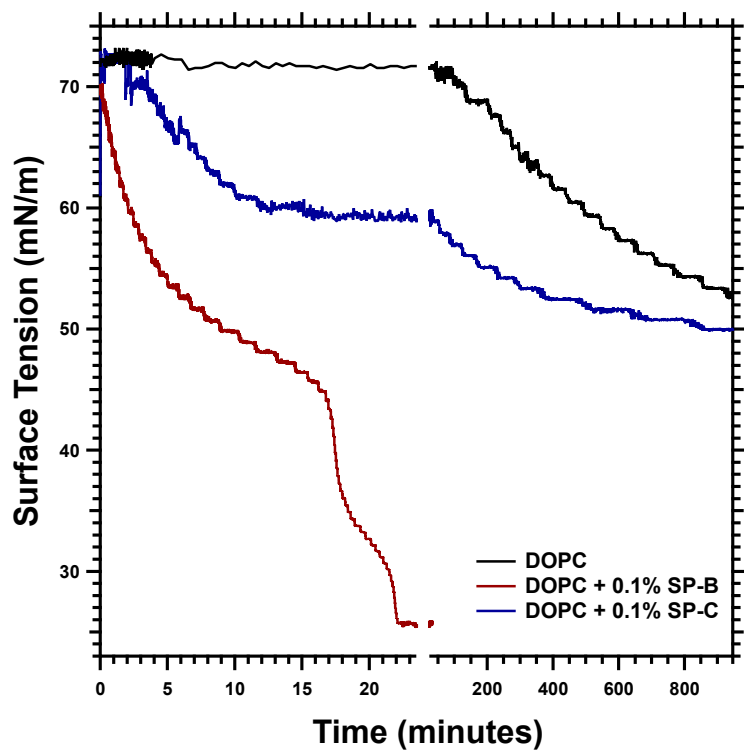
Air

Water

R_1

R_2

Vesicle

Figure 1

A. Non-reducing

SP SP-B SP-C MWM

B. Reducing

SP SP-B SP-C MWM Mol. Wt. (kDa)

30

20

15

10

Fig. 3

Figure 4

A. POPE ± SP

% SP
○ 0.00
□ 0.01
△ 0.03
▽ 0.10
◁ 0.30
▷ 1.00
◇ 3.00
◇ 5.00

Q_{II}^P

Q_{II}^D

L_β

L_α

H_{II}

B. POPE ± SP-B

% SP
○ 0.00
△ 0.03
▽ 0.10
◁ 0.30
▷ 1.00
◇ 3.00
◇ 5.00

C. POPE ± SP-C

% SP
○ 0.00
△ 0.03
▽ 0.10
◁ 0.30
▷ 1.00

a_o, nm

Temperature, °C

Figure 5

Figure 6